IJCRT.ORG ISSN : 2320-2882

INTERNATIONAL JOURNAL OF CREATIVE RESEARCH THOUGHTS (IJCRT)

An International Open Access, Peer-reviewed, Refereed Journal

Dielectric properties and physical properties of Pure and Nano Ag Doped Liquid Crystalline Compounds

Dr. Gajendra Prasad Gadkar

Associate Professor

Department of Physics

College of Commerce, Patliputra University

Abstract

This paper reveals that the dielectric properties and other physical properties, for example, electrical conductivity (AC) and unwinding time or initiation vitality have been read for two frameworks unadulterated LC [V]6,6, [V]7,6, [V]8,6, [V]6,7, [V]7,7 and [V]8,7 and their doped with silver nanoparticles. The outcomes show the expanding in genuine dielectric permittivity έ with expanding length terminal chain. So the genuine dielectric permittivity expanding with raising temperature. To think about between the estimations of (400) Hz and (4000) Hz we watch these qualities at the low recurrence are bigger than that in high recurrence. By and large, one can see that the doping of Ag nano particles viably diminished the permittivity of the LC materials with its huge electric dipole second. The electrical conductivity σ esteem for unadulterated LC tests as a rule increments with expanding temperature. So we watched expanding of electrical conductivity esteems at high recurrence. The time scale is talked about as far as the Arrhenius plot. For the most part, with expanding the temperature the timeframe that spends by atoms at the change state will increment. The initiation vitality Ea esteems show the expansion in the enactment vitality to the doped frameworks.

Keywords: Liquid crystals; Dielectric permittivity; Electrical conductivity; Relaxation time; Activation energy; Doped liquid crystals; Silver nanoparticles

Introduction

The significance of fluid gems lies in their broad use in show gadgets, it is notable that fluid gems are extremely delicate to an electrical field. This property permits their applications to shows and other optical gadgets innovation [1-5]. Anyway the utilization of fluid precious stones in various devises relies on different properties claimed by them like request boundary, dielectric permittivity, dielectric anisotropy, birefringent conduct, optical transmittance, flexible constants and so forth [6]. Most utilizations of fluid precious stones rely on the potential outcomes of changing direction of the fluid gem atoms by the applied electric fields, which thus relies upon the visco-flexible and electrical properties [7-9].

A specific utilization of fluid gems requires a specific arrangement of boundaries of the fluid precious stone in required range. The dielectric considers have been valuable as they give significant data in regards to sub-atomic structure, sub-atomic elements, and kind of sub-atomic connections in the example [6]. The idea of nanomaterials might be leading, semiconducting, dielectric, protecting, natural, inorganic and is accessible in various sizes and shapes like round, wires, tubes, bars and so on [10,11].

Fluid gems are significant materials due to their logical and mechanical significance, yet a solitary fluid gem material can't satisfy all the prerequisites for a handy gadget. Thusly, the various blends of fluid precious stones and their doped examples have increased developing interest. These doped examples have rising possibilities with respect to their applications in data handling [12].

In the current paper, our point is to concentrate some physical properties, for example, dielectric permittivity, electrical conductivity and unwinding time or enactment vitality for two frameworks unadulterated LC [V]6,6, [V]7,6, [V]8,6, [V]6,7, [V]7,7 and [V]8,7 and their doped with silver nanoparticles. The general structure of mixes have been considered is appeared in (Figure 1). The entirety of the mixes in both two arrangement [V]m,6 and [V]m,7 show mesomorphic properties. All individuals from those two arrangement display an enantiotropic dimorphism smectic A (SmA), smectic C (SmC) and additionally nematic (N) stages.

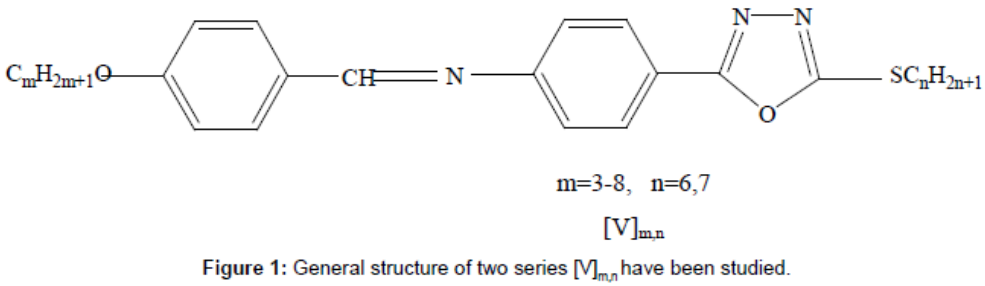

Figure 1: General structure of two series $[V]_{m,n}$ have been studied.

Figure 1: General structure of two series $[V]_{m,n}$ have been studied.

Experimental Materials

Fluid crystalline mixes which considering were blended and distributed in our past work [13]. Ceaselessly, to improve the physical investigation, Silver nanoparticles were set up by decrease technique and recognized by for the most part examination XRD, SEM and AFM. From these methods the molecule size of nano appeared to be under 50 nm.

Instrumentation

Dielectric permittivity estimations:

The dielectric conduct of the materials has been concentrated by utilizing an instrument to quantify dielectric consistent LCR meter (hp-4274A) multi-recurrence, based warming gadget hot stage polarizing magnifying lens. The dielectric boundaries have been estimated as a component of temperature go 90°C-160°C at 400 Hz and 4000 Hz. The examples warmed to arrive at isotropic stage, at that point cooled the boundary of dielectric steady and opposition have been recorded each 10°C.

Planning of cells:

Two comparative cells having dynamic zones of 1 cm2 were set up by utilizing straightforward and profoundly leading ITO (indium tin oxide) covered optically level glass substrates utilized as terminals. These anodes give a base to the LC test to adjust. Planar arrangement is acquired by rewarding with both a grip advertiser and a polymer (polyimide PI2555) and afterward scoured unidirectionally with a velvet material. The thickness of the cell was kept up at (12 μm) by methods for mylar spacers. The right and legitimate arrangement of the LC particles is critical for exact

estimation of electrical properties, which thusly impacts the dielectric boundaries and in this way assumes a critical job in atomic geometry.

Planning of tests:

Sandwich cells have been warmed on hotplate delicately after that materials affected by narrow activity. That is for unadulterated LC tests, while for LC doping silver nano molecule tests, take 0.1 gm of LC then blended in with 0.025 gm from silver nano molecule in 15 mL of benzene as a dissolvable. The arrangement meant ultrasonic instrument under 6 power to annihilate conglomerations, let dissolvable to dissipate then the doping frameworks was gathered and affected similarly.

Arrangement of silver nano particles:

Silver nitrate AgNO3 and trisodium citrate C6H5O7Na3 of investigative evaluation virtue were utilized as beginning materials. The silver colloid was set up by utilizing compound decrease strategy [14]. All arrangements of responding materials were set up in refined water. In run of the mill test 250 mL of 0.01 M AgNO3 was warmed to bubbling. To this arrangement 25 mL of 5% trisodium citrate was included drop by drop. During the procedure arrangement was blended vivaciously and warmed until shading's change is clear (light yellow). At that point it was expelled from the warming component and blended until cooled to room temperature, Ag nano particles were gathered and washed commonly [15]. Substance condition of the response could be express as follows [16,17]

$$4Ag^{+} + C_6H_5O_7Na_3 + 2H_2O \rightarrow 4Ag0 + C_6H_5O_7H_3 + 3Na^{+} + H^{+} + O_{2\uparrow}$$

Portrayal of silver nano particles:

Portrayal of nanoparticles is imperative to comprehend and control nanoparticles combination and applications. Portrayal is performed utilizing a wide range of procedures, for example, powder X-beam diffractometry (XRD), filtering electron microscopy (SEM) and nuclear power microscopy (AFM). These methods are utilized for assurance of various boundaries, for example, molecule size, shape and crystallinity. For example, the morphology and molecule size could be dictated by SEM and AFM. The benefit of AFM over conventional magnifying instruments, for example, SEM is that AFM estimates three-dimensional pictures with the goal that molecule stature and volume can be determined. Additionally, X-beam diffraction is utilized for the assurance of crystallinity [17].

XRD investigation:

In Figure 2 shows the XRD example of powder silver nano molecule. There is nearness of three biggest tops at 2ɵ values 38.1203, 44.2895 and 64.4542. In this manner, the XRD range affirmed the crystalline structure of silver nano particles. All the tops in XRD example can be promptly filed to a face-focused cubic structure of silver. In any case, the diffraction tops are expansive which showing that the crystallite size is little. The nano molecule size (L) has been determined by Deby Scherrer's recipe [18].

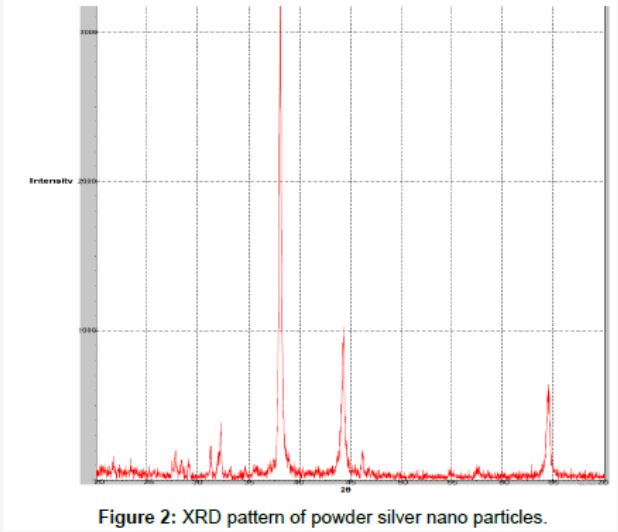

Figure 2: XRD pattern of powder silver nano particles.

Figure 2: XRD pattern of powder silver nano particles.

$$L = \frac{0.94\lambda}{\beta\cos\theta} \quad (1)$$

Where λ is wave length 0.167 A0 of X-rays used, β is broadening of diffraction line measured at half of its maximum intensity (in radian) and ɵ is Bragg's diffraction angle (in degree). The crystallite size of silver nano particles have been found to be 49.18 nm, 33.88 nm and 19.41 nm.

SEM analysis:

Scanning electron microscopy has provided further insight into the morphology and size details of the synthesized silver nano particles are shown in (**Figure 3**). The large aggregation was found attributed to not using a disperser in the techniques

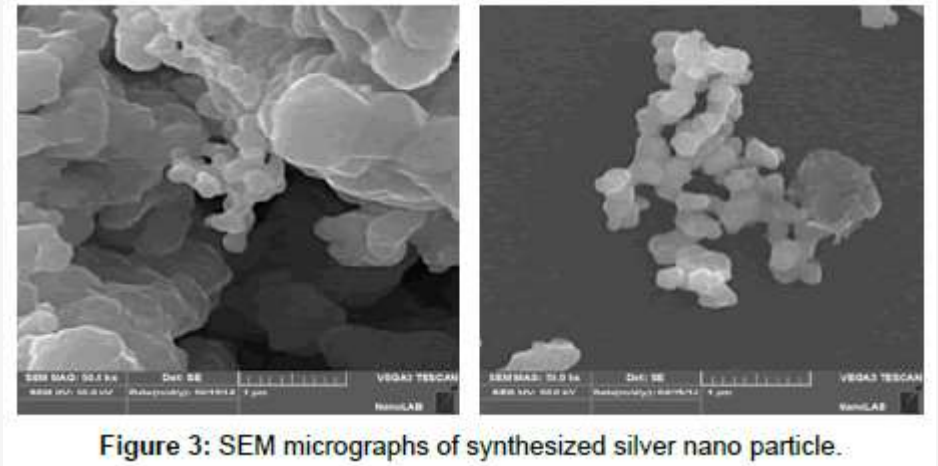

Figure 3: SEM micrographs of synthesized silver nano particle.

Figure 3: SEM micrographs of synthesized silver nano particle.

AFM analysis:

Atomic force microscopy indicates particles and distribution average size, which was less than 50 nm as shown in (**Figure 4**).

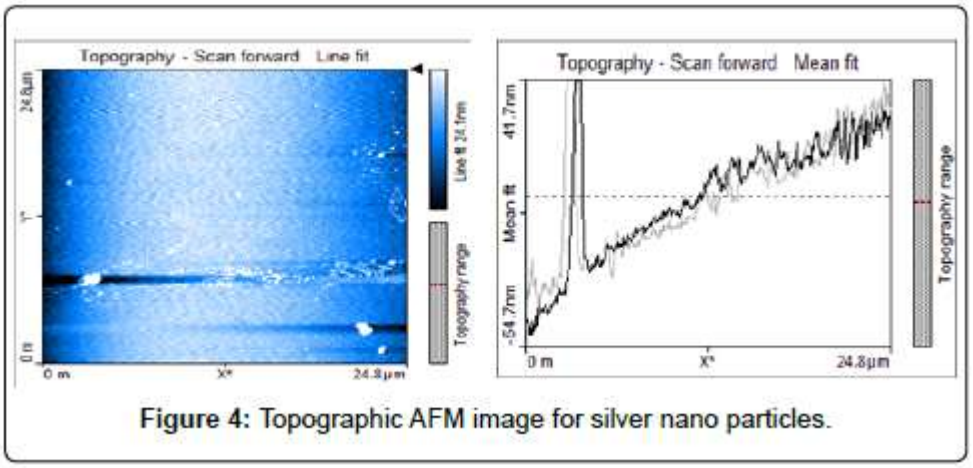

Figure 4: Topographic AFM image for silver nano particles.

Results and Discussion

Dielectric permittivity properties

Measured quantities were the capacitance (C_x) and resistance (R) of the specimen, so real dielectric permittivity (έ) and imaginary dielectric permittivity (ε") were calculated as follow equations [19-21].

$$\acute{\varepsilon} = \frac{C_x}{C_a} \quad (2)$$

$$\tan\delta = \frac{1}{\omega.R.C_x} \quad (3)$$

$$\varepsilon'' = tan\delta.\acute{\varepsilon} \quad (4)$$

where C_a is the capacitance of the cell with air which is equal to (0.0885)A/t; A is the area of the electrode in m2, which equal 0.001 m2 and t is the thickness of the specimen in m, which equal 12 μm. C_x is the electrostatic capacity of the specimen in pf, R is the resistance of the specimen and ù = 2ðf , f; is the applied frequency. In the present investigation, two types of cells were prepared, one for pure LC material and another one with Ag nanoparticles doped LC material, for comparative study. In **Figures 5** and **6** shows the temperature dependence of real dielectric permittivity έ for the pure liquid crystalline samples at frequency 400 Hz and 4000 Hz. While **Figures 7** and **8** shows the temperature dependence of real dielectric permittivity έ for pure liquid crystalline and nano Ag doped liquid crystalline $[V]_{8,6}$ and $[V]_{8,7}$ samples (as a representative examples) at frequencies 400 Hz and 4000 Hz, the characteristic features of these measurements can be listed as follow:

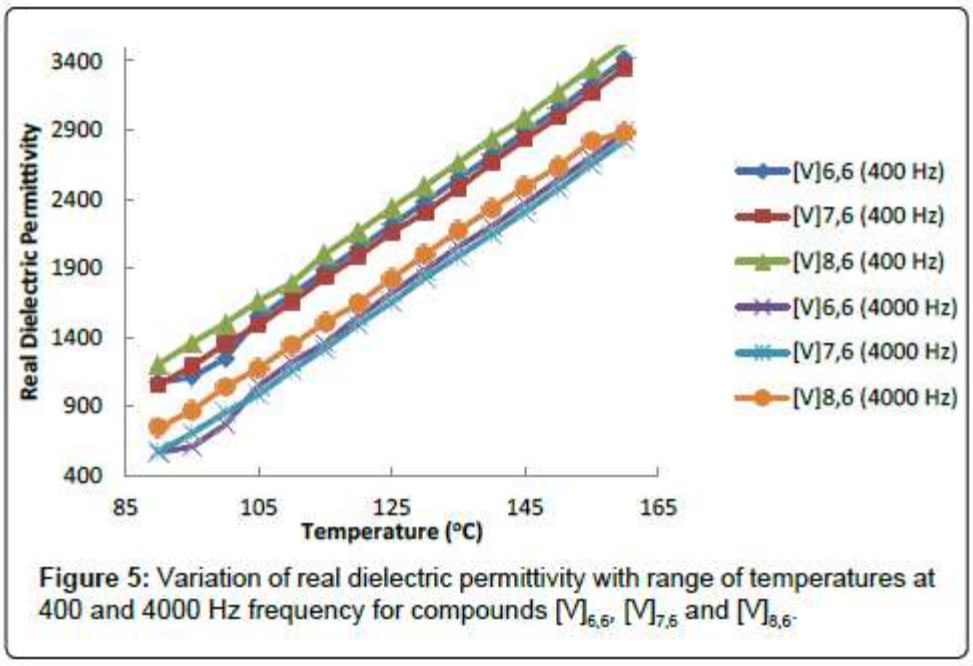

Figure 5: Variation of real dielectric permittivity with range of temperatures at 400 and 4000 Hz frequency for compounds $[V]_{6,6}$, $[V]_{7,6}$ and $[V]_{8,6}$.

Figure 5: Variation of real dielectric permittivity with range of temperatures at 400 and 4000 Hz frequency for compounds $[V]_{6,6}$, $[V]_{7,6}$ and $[V]_{8,6}$.

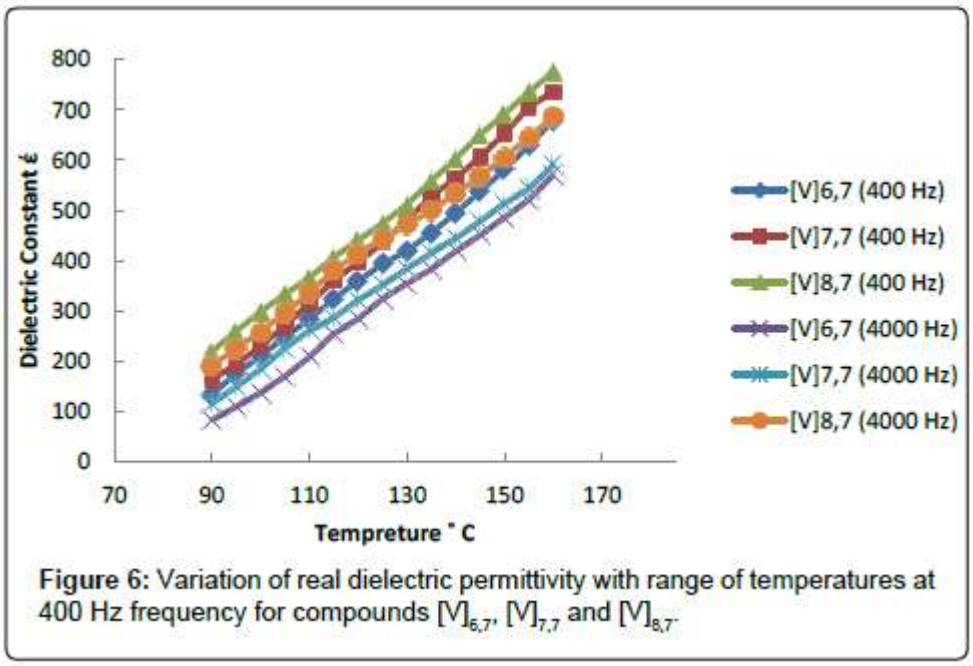

Figure 6: Variation of real dielectric permittivity with range of temperatures at 400 Hz frequency for compounds $[V]_{6,7}$, $[V]_{7,7}$ and $[V]_{8,7}$.

Figure 6: Variation of real dielectric permittivity with range of temperatures at 400 Hz frequency for compounds $[V]_{6,7}$, $[V]_{7,7}$ and $[V]_{8,7}$.

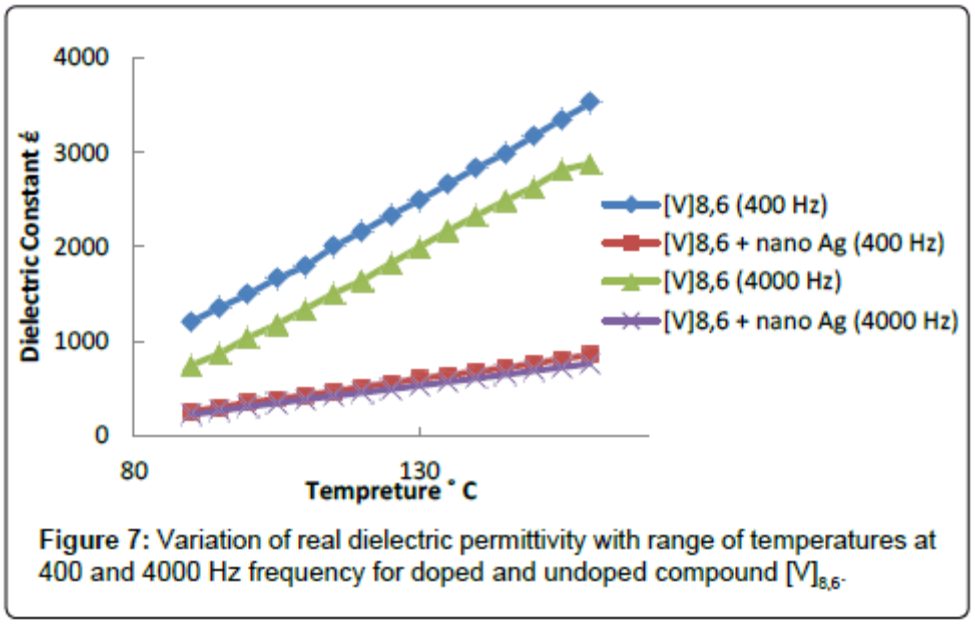

Figure 7: Variation of real dielectric permittivity with range of temperatures at 400 and 4000 Hz frequency for doped and undoped compound $[V]_{8,6}$.

Figure 7: Variation of real dielectric permittivity with range of temperatures at 400 and 4000 Hz frequency for doped and undoped compound $[V]_{8,6}$.

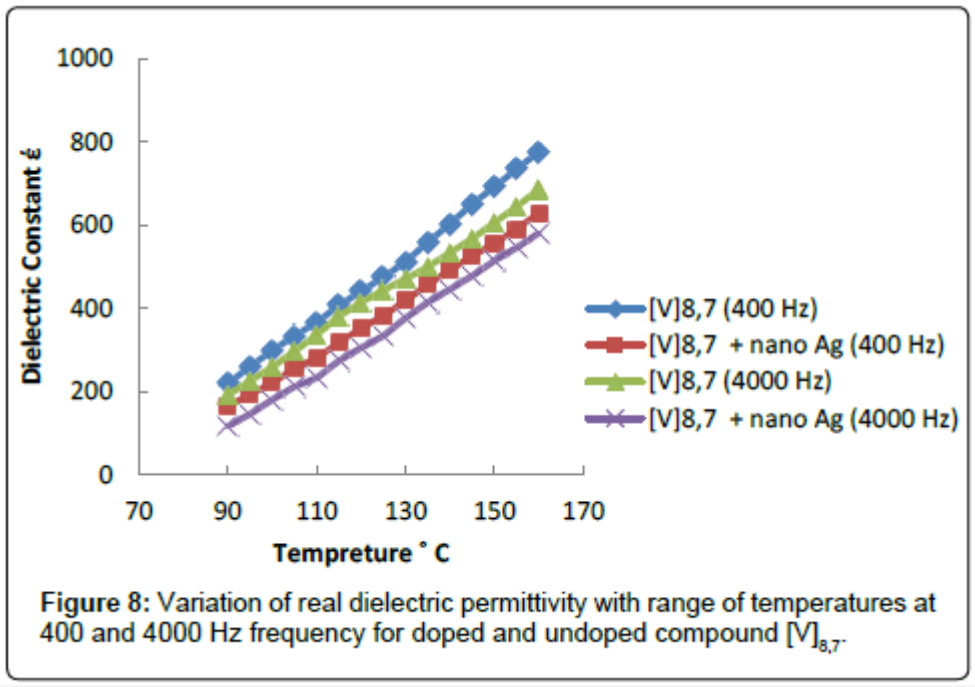

Figure 8: Variation of real dielectric permittivity with range of temperatures at 400 and 4000 Hz frequency for doped and undoped compound $[V]_{8,7}$.

Figure 8: Variation of real dielectric permittivity with range of temperatures at 400 and 4000 Hz frequency for doped and undoped compound $[V]_{8,7}$.

1. In all figures έ increments with expanding temperature at the two frequencies.

2. In the both arrangement [V]m,6 and [V]m,7 at all temperature extend the estimation of έ at 400 Hz is bigger than that at 4000 Hz.

3. There is an expansion in έ esteem with expanding length of the alkyl side chain in the two frequencies for every single unadulterated example.

4. The estimation of έ for [V]m,6 is bigger than that of [V]m,7.

5. Expansion of Ag nano particles acts to diminish esteem impressively.

In arrangement [V]m,6 there is an extraordinary change in warm coefficient dέ/dT among doped and undoped tests, however in [V]m,7 arrangement this coefficient is roughly in doped and undoped tests.

There is no impressive change in dέ/dT by changing from strong precious stones to fluid crystalline mesophase then to isotropic stage.

The main point in the above rundown can be portrayed as follows: one of the implications of genuine dielectric permittivity is the inclination of the perpetual or prompted dipole snapshot of the atomic framework to arrangement with applied electrical field. From this view point we can portray the genuine dielectric permittivity conduct with temperature as follow, at low temperatures when the measomorphic mixes at strong express the warm movement of the particles can't mastermind with applied field however with expanding temperature during the progress to mesomorphic stage, the expanding warm movement of the atoms free these particles and give their greater capacity to connect with differing electrical field.

To analyze between the estimations of έ at 400 Hz and 4000 Hz we watch these qualities at the low recurrence are bigger than that in high recurrence, this demonstrate warm movement of atoms can join with applied electrical field at low recurrence 400 Hz, while at higher recurrence 4000 Hz this movement can't follow the pace of changing field, as appeared in past figures. The expanding in genuine dielectric permittivity έ with expanding length terminal chain is because of the hydrophobic practices (less polarizability), translation of the connection of long the side chain of the terminal gatherings and the benefit of as per the law [22]

$$\mu = q \cdot d \quad (5)$$

Where, μ is the electric dipole second. In the straightforward instance of two point charges, one with charge +q and the other one with charge – q while d is the uprooting vector pointing from the negative charge to the positive charge. The expansion of the separation between inverse charges will expand the dipole second worth (prompted or lasting), so that έ will increment.

The dropping of έ esteem within the sight of Ag nanoparticles is clarified in the light of that dielectric medium have dipole second and direction polarization (nuclear polarization and electronic polarization) [15], that the space charge thickness is higher at lower recurrence in the mass just as close to the surfaces. With expanding the recurrence the space charge thickness is diminished in the mass just as close to the surfaces. In this way, at lower recurrence the space charge impact is predominant. When nano particles were doped into the LC framework, the direction of nano molecule was with the end goal that the dipole snapshot of nano particles are contradicting the dipole snapshot of LC atom and that dielectric steady reductions for nano doped frameworks [19]. Same figures show the connection between the dielectric permittivity and temperature for unadulterated LC and Ag nano particles doped LC framework in a 400 Hz and 4000 Hz recurrence. The dielectric permittivity has expanded definitely with builds temperature. We can see from figures that there is enormous contrast in the dielectric permittivity for unadulterated LC and Ag nano particles doped LC frameworks. Indicate can't help thinking that nano particles are broken the balance of LC atom, the dipole snapshot of nano particles are hostile to resemble bearing of the dipole snapshot of LC particle [23]. Along these lines, we can see that the doping of Ag nano particles viably diminished the dielectric permittivity of the LC materials with its enormous electric dipole second.

Nonexistent dielectric permittivity

The genuine dielectric permittivity property of the medium is a boundary of how much vitality from an outer electric field is put away in a material, while fanciful dielectric permittivity or the misfortune edge is a boundary of the lost vitality by the field when this outside field is reflect [24].

The misfortune digression or tan δ is characterized as a proportion of the nonexistent piece of the dielectric permittivity to the genuine part. The nonexistent dielectric permittivity is a proportion of lost vitality of the wavering electrical field that happened when electrical minutes inside the encasing go to follow the swaying applied electrical field [24]. As we see beforehand the expanding of temperature act to empower the atomic minutes to follow the

applied electrical field, then again expanding of temperature act likewise to build the irregular movement of the particles also, so there will be an amount of electrical field vitality devoured to compose the arbitrary coordinated sub-atomic electrical minutes toward the applied field. In Figures 9 and 10 show the temperature reliance of nonexistent dielectric permittivity or dielectric misfortune factor ε" of unadulterated fluid crystalline and nano Ag doped fluid crystalline [V]6,6 and [V]7,7 (as a delegate models) tests at 400 Hz and 4000 Hz. These practices can be summed up as:

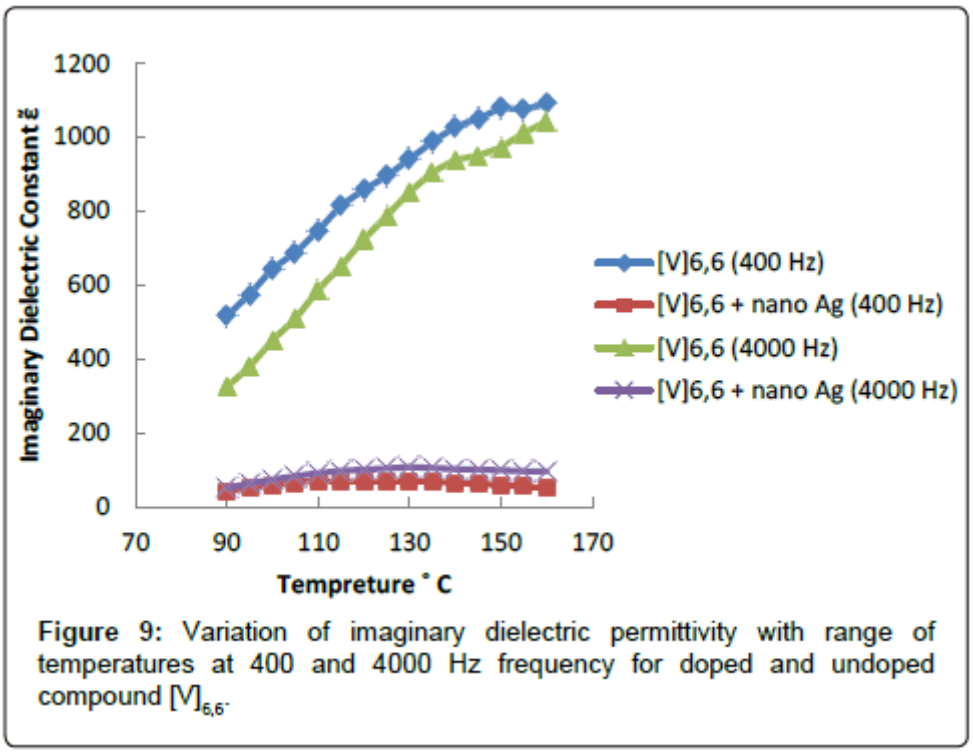

Figure 9: Variation of imaginary dielectric permittivity with range of temperatures at 400 and 4000 Hz frequency for doped and undoped compound $[V]_{6,6}$.

Figure 9: Variation of imaginary dielectric permittivity with range of temperatures at 400 and 4000 Hz frequency for doped and undoped compound $[V]_{6,6}$.

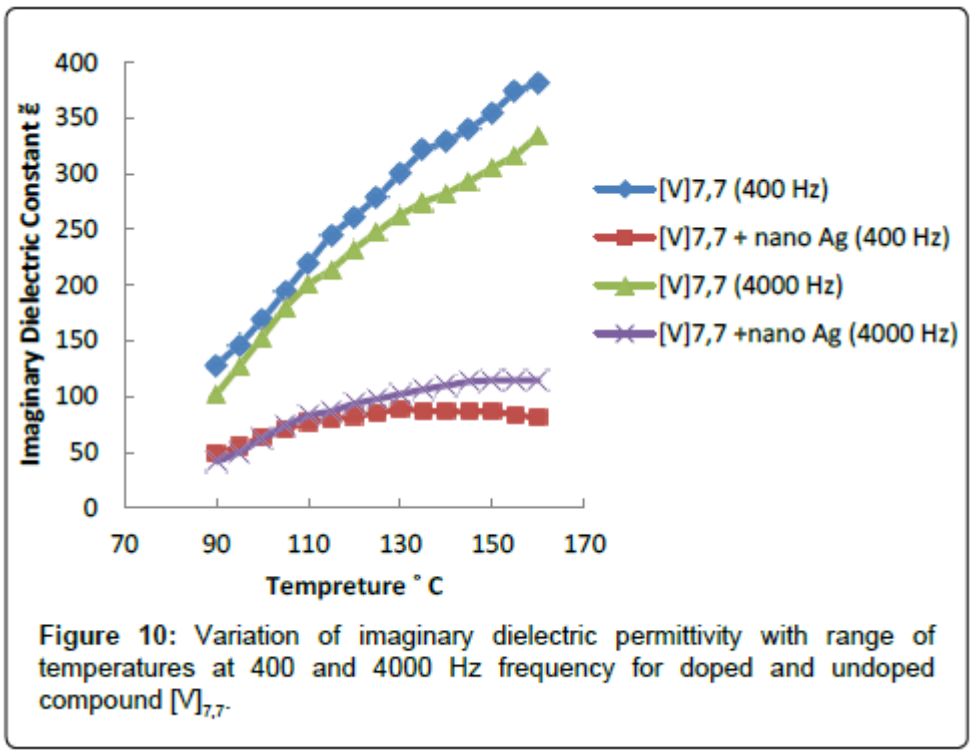

Figure 10: Variation of imaginary dielectric permittivity with range of temperatures at 400 and 4000 Hz frequency for doped and undoped compound $[V]_{7,7}$.

Figure 10: Variation of imaginary dielectric permittivity with range of temperatures at 400 and 4000 Hz frequency for doped and undoped compound $[V]_{7,7}$.

1. For unadulterated examples ε" increments with expanding temperature however in a non-straight way where is there are purposes of brokenness of warm coefficient dέ/dT with expanding temperature.

2. ε" values at 400 Hz are more prominent than that at 4000 Hz aside from [V]m,7 arrangement where its qualities at 400 Hz cover in a wavering structure with that at 4000 Hz.

3. With expanding length of the side chain of both arrangement the warm coefficient dέ/dT diminishes while by examination between the two arrangement the estimation of ε" for [V]m,6 arrangement is more prominent than that of [V]m,7 arrangement.

4. For doped examples the estimations of ε" are littler than that for unadulterated examples and furthermore they have a low estimation of dέ/dT relative with unadulterated examples. With expanding length of the side chain there is a clear diminishing of ε" values in both arrangement lastly ε" values for [V]m,6 arrangement are bigger than that of [V]m,7 arrangement.

The non-direct reaction of ε" with temperature shows that ε" is more delicate to the stage changes than ε" where the brokenness focuses on the bend have a place with the progress temperatures of the LC material this affectability might be because of nature of the lost vitality by the field which identified with the entropy of change. For the most part, with expanding temperature at the two frequencies watch expanding of nonexistent dielectric steady qualities with expanding temperature accordingly to build the irregular direction of sub-atomic minutes with expanding temperatures, which act to scatter or expend progressively lost vitality to situate these minutes with applied outside field. This case is clear in unadulterated LC frameworks, while in doped Ag nano LC frameworks, the warm coefficient dέ/dT of this procedure is littler than that in unadulterated examples. The explanation of this because of the sharp decrease of the quantity of sub-atomic minutes and sub-atomic portability also which brought about by the expansion of Ag nano particles that withdraw the sub-atomic versatility through electrostatic twofold layer that extinguish the sub-atomic dipoles of LC. These variables will in general abatement this warm reaction in the two states (diminishing or expanding with temperatures).

In examination between ε" values at 400 Hz and 4000 Hz we watch these qualities is by all accounts near one another which doesn't concur with ε " values at these various frequencies, those the έ values at 400 Hz is more noteworthy than that at 4000 Hz, this might be because of that the lost vitality that communicated by ε" is rely upon the warm vitality more than its reliance on the applied outer field, so we are imagine that ε" is identified with entropy of the framework with loser connection. Notwithstanding, the nonexistent dielectric permittivity have marginally lower esteems at 4000 Hz from that 400 Hz, this because of the particles have not capacity to stream the substituting electrical field at high recurrence, so the lost vitality that expended during the variation procedure will be little. While at 400 Hz the atoms of the medium can substitute, the amount of the lost vitality will be bigger than that in 4000 Hz.

For doped examples the estimations of ε" are littler than that for unadulterated examples and furthermore they have a low estimation of d relative with unadulterated examples with expanding length of the side chain there is a clear reduction of ε" values in both arrangement lastly ε" values for [V]m,6 arrangement are bigger than that of [V]m,7 arrangement.

We can clarify the diminishing of fanciful dielectric permittivity in the doped frameworks by that the doped Ag nano particles through its charge surface which naturalize the dipole snapshot of LC atoms, so there will be incredible breakdown in dielectric property of medium as aftereffect of presence of enormous surface territory to nano particles and consequently the surface charges or electrostatics twofold layers go about as retarder extinguishing factors for the sub-atomic dipole minutes and in this manner the over all ε" of medium will be low. In the doped Ag nano particles frameworks as we see before act to limit the versatility of atoms and extinguish their dipole minutes, thus the lost vitality by the field will be a low at both two frequencies on account of the quantity of dipoles that can stream the rotating field will be to a great extent diminished. As exceptional case in [V]8,7, we see the fanciful dielectric permittivity has low qualities in the two frequencies so the distinctive is extremely little between 400 Hz and 400 Hz, we can presume that the expanding in the terminal chain act to permit the atomic minutes follow the substituting outer field in the two frequencies too, so the estimation of έ and ε" in shut to one another in unadulterated materials.

Electrical conductivity

Electrical conductivity (AC) values have been determined by following condition [25]:

$$\sigma_{ac} = \varepsilon_0 \varepsilon'' \omega \quad (6)$$

where ε0 is the free space dielectric permittivity ($8.85*10^{-12}$) F/m, ε'' is imaginary dielectric permittivity, ω is the angular frequency of applied electric field, which equal (2πf). In **Figures 11** and **12** show the variation of σ values with the temperatures at two frequencies for doped and pure liquid crystalline $[V]_{6,6}$ and $[V]_{8,7}$ (as a representative examples) samples.

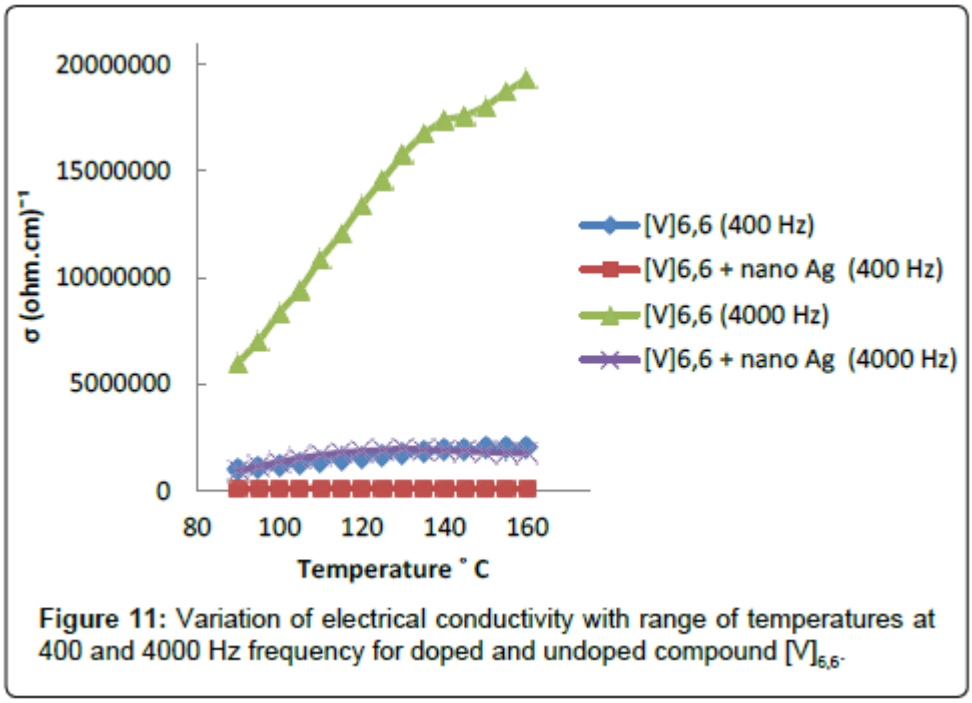

Figure 11: Variation of electrical conductivity with range of temperatures at 400 and 4000 Hz frequency for doped and undoped compound $[V]_{6,6}$.

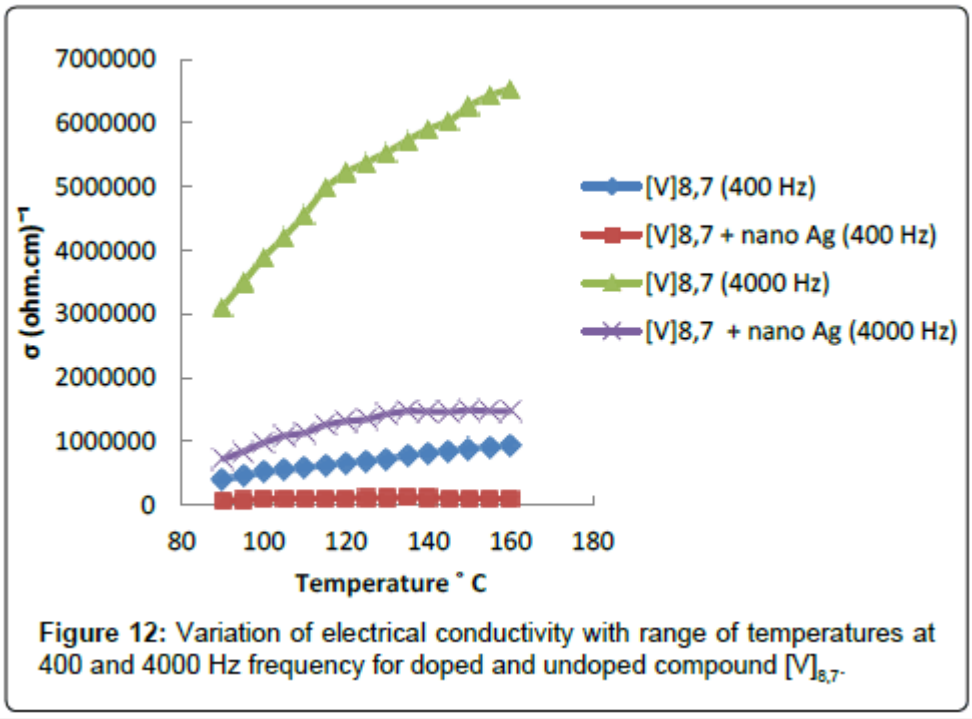

Figure 12: Variation of electrical conductivity with range of temperatures at 400 and 4000 Hz frequency for doped and undoped compound $[V]_{8,7}$.

Figure 12: Variation of electrical conductivity with range of temperatures at 400 and 4000 Hz frequency for doped and undoped compound $[V]_{8,7}$.

The trademark highlights of these figures are:

1. Electrical conductivity σ increments with temperature like ε" in a non-straight structure.

2. The estimation of σ at 4000 Hz is more noteworthy than that at 400 Hz, the warm coefficient of σ dσ/dT at 4000 Hz is additionally more prominent than that at 400 Hz.

3. σ and dσ/dT decline with expanding length of alkyl side chain at the two frequencies.

4. In doped examples σ is lower than that of unadulterated examples what's more σ at 400 Hz is close in worth and incline dσ/dT to the σ of doped examples at the two frequencies.

The conductivity esteem for all examples is ordinary for semi-conductors [24]. For unadulterated LC tests as a rule there are an expansion in σ esteem with expanding temperature, this is ordinary as indicated by Boltzman law condition (6) [26]:

$$\sigma = \sigma_{\circ} e^{-Ea/k_B T} \quad (7)$$

Where σ° is the pre-exponential factor, Ea is the enactment vitality, kB is Boltzmann's consistent and T is the supreme temperature. Which shows that materials like covers, semi-directors and ionic directors the temperature demonstrations to build the quantity of charge transporters through furnishing these bearers with vitality that required to cross the band hole among comparable and leading groups. The nonlinear expanding of electrical conductivity demonstrates its affectability to stage changes that occurring to the example with expanding temperature [24].

To clarify the distinction of σ and its warm angle at the two frequencies we have to concentrate on component of charge transport, σ is relying upon two factors the first is the quantity of charge bearers, the subsequent one is the portability of these bearers. At 400 Hz warm conductance increment with temperature yet in less angle factor than that of 4000 Hz the explanation can be depicted by the charge versatility factor not by number of charge type, in strong state charge moved by three instrument the first is the exchange from a conductance band to other neighboring band in covering with initial one, this system accurse in run of the mill directors. The subsequent component occur when there

are a likely boundary between the conductance band and its neighboring conductance groups however this potential is little so the charges can bouncing from conductance band to its neighbors. The third component is a passage impact instrument which is occurring when the potential hindrance is more prominent than the charge active vitality. This instrument has an extremely little commitment to the charge versatility [24]. From above conversation we can reason that the low slope estimation of warm conductivity at 400 Hz is because of the difference in portability of the charge bearers through the bouncing instrument and not by the expanding number of charge transporters which is create through expanding temperature. From similar figures, we can watch expanding of electrical conductivity esteems at high recurrence, this can be clarified by that when field swaying time is a lot littler than the unwinding time of the substance, at that point the ionic air around the charge transporters can't follow the moving charge bearer is all the more free in development with wavering field, this procedure is occurred in both doped and unadulterated LC frameworks too.

The impact of expanding length of the side chain on σ and dσ/dT is the diminishing them two the decline of σ occurred because of expanding of the hydrophobic character of the substance which lessens σ esteem. The abatement of dσ/dT originates from expanding the separation among directing groups through the expanding of atomic length which act to raise the vitality hindrance among the directing groups and prompts decline the likelihood of intersection the charge bearer through jumping system among leading groups.

Notwithstanding that past clarification, we can presume that the silver nano particles in a lattice of LC materials go about as a snare to charge brings through two different ways, the first by acting of gathering the free electrons in the leading groups that described its metallic nature, these nano particles of silver is by all accounts isolated as islands which the charge move by them through jumping component. The second method of catching charge transporters originate from the high surface territory of nano frameworks and electro static twofold layer of these surfaces which search any free charge exist.

Unwinding time and actuation vitality

The term unwinding time implies the timespan beginning from the arrangement of an atomic conglomeration until its vanishing, this term is utilized oftentimes to depict a condition of measurable harmony of the framework and the pace of the presence of this balance is connected with change likelihood of that framework from introductory balance state to another balance state. On account of dielectric estimations the main harmony state depict the atomic design without electrical field while the subsequent balance state portray the sub-atomic setup within the sight of the electrical field. Likewise unwinding time is determined from the condition (7) [27].

The temperature reliance of unwinding time adheres to Arrhenius law which is given by condition (8) [27-29]:

$$\tau = \tau_0 e^{-Ea/k_B T} \quad (8)$$

Where Ea is the enactment vitality, τ0 is the pre-exponential factor kB is Boltzmann's consistent and T is the supreme temperature. The Arrhenius condition portrays the conduct for a procedure starting with one state then onto the next isolated by an expected boundary and the tallness of the obstruction deciphers the initiation vitality [29]. By and large at low estimations of Ea or at high temperatures the unwinding time will be little in light of the fact that the particles will have enough vitality to cross the boundary of initiation vitality from starting arrangement to the second setup in this way the procedure will be quick or the unwinding time will be little, so the circumstance is turned around at high estimations of Ea or at low temperatures which the procedure will be moderate and the framework will require more opportunity to move from design to other one.

$$\tau = 1 / 2\pi f.\tan\delta \quad (9)$$

In **Table 1** indicates the value of activation energy calculated from the slope of the ln τ versus 1/T plot (figures not shown) that required to transforming of the molecular configuration at tow electrical field frequencies for pure liquid crystalline and Ag nano particle doped samples, this table shows the following:

Samples	Ea (J/mol)400 Hz	Ea (J/mol) 4000 Hz	Samples	Ea(J/mol) 400 Hz	Ea (J/mol) 4000 Hz
$[V]_{6,6}$	670.7	677.0	$[V]_{6,6}$+Nano Ag	2357.9	1538.9
$[V]_{7,6}$	864.7	888.7	$[V]_{7,6}$+Nano Ag	3347.2	2158.8
$[V]_{8,6}$	1112.4	1151.4	$[V]_{8,6}$+Nano Ag	4873.7	2816.8
$[V]_{6,7}$	721.9	749.4	$[V]_{6,7}$+Nano Ag	1302.8	1229.6
$[V]_{7,7}$	707.4	774.1	$[V]_{7,7}$+Nano Ag	1674.4	1308.0
$[V]_{8,7}$	697.0	897.1	$[V]_{8,7}$+Nano Ag	1805.0	1520.6

Table 1: Activation energy values for pure LC and nano Ag doped samples.

1. Actuation vitality Ea for doped examples are more prominent from that for unadulterated examples.

2. For all arrangement at all frequencies Ea increments with expanding length of the side chain aside from arrangement [V]m,7 at 400 Hz which show a contrary conduct.

3. For unadulterated examples Ea esteem at 4000 Hz is bigger than that in 400 Hz, this case is turned around for doped examples where Ea esteem at 4000 Hz is littler than that in 400 Hz.

The expansion in the initiation vitality of the doped examples might be because of the confining of the conformational movements that occurred in LC terminal chain materials or lessening the portability of these atoms through the cooperation (adsorption) with the outside of nano particles.

With expanding length of the side chain we expect expanding the unwinding time that required to restoring a balance setup and the expansion of τ esteem show up as increment in Ea esteem, the explanation is because of the expansion of interior degrees of opportunity of the atoms and raising the probabilistic number of compliances which the LC particle can have before arriving at the ideal one that is essential for setting up the harmony. For [V]m,7 arrangement the unusual conduct at these frequencies is have a place with similar reasons that showed up by this arrangement in past estimations.

Conclusion:

Because of the symphonious reaction of LC atoms in the unadulterated examples with applied electrical at 400 Hz the enactment vitality will be not as much as that at 4000 Hz in light of the fact that the speed period time of exchanging field don't give enough an ideal opportunity for the LC particles to follow its shift, along these lines initiation vitality at high recurrence 4000 Hz will be not as much as that at low recurrence 400 Hz, the LC particles are in consonant development with applied field at 400 Hz however this movement are stacked with massive Ag nano particles so its require more vitality to affirm this consonant movement this prompts the LC particles which don't reaction well with applied field at 4000 Hz need a lower vitality to arrive at the balance when the LC particles doped with Ag nano particles.

References

1. Dunmur DA (2002) Liquid Crystals: Fundamentals, World Scientific, New York, USA.

2. Gray GW, Hird M, Lacey D, Toyne KJ (1989) The synthesis and transition temperatures of some 4,4"-dialkyl- and 4,4"-alkoxyalkyl-1,1':4',1"-terphenyls with 2,3- or 2',3'-difluoro substituents and of their biphenyl analogues. J ChemSoc Perkin Trans 2: 2041.

3. Cosquer GY (2000) Liquid Crystals with Novel Terminal Chains as Ferroelectric Hosts, PhD Thesis, University of Hull, England.

4. Glendenning M (1998) Liquid Crystalline Materials for Ferroelectric Mixtures of High Dielectric Biaxiality. PhD Thesis, University of Hull, England.

5. Hall DG (2005) Boronic Acids: Preparation, Applications in Organic Synthesis and Medicine. WILEY-VCH Verlag GmbH & Co. KGaA, Weinheim.

6. Taraka N, Rao R, Raju R, Sita A, Venkayya P (2014) Thermodynamical, dielectric and optical properties of liquid crystal sample signallingSmA point. African Journal of physics 2: 7.

7. Strangi G , Cazzanelli E, Scaramuzza N, Versace C, Bartolino R (2000) Electrical and electro-optical investigations of liquid crystal cells containing WO3 thin films.Phys Rev E Stat Phys Plasmas Fluids RelatInterdiscip Topics 62: 2263-2268.

8. Yadav SP, Pandey KK, Misra AK, Manohar R (2011) Electro-optical behavior of dye doped Nematic liquid crystal.ActaPhysicaPolonicaA 119: 824.

9. Manohar R, Tripathi G, Misra AK, Srivastava AK, Shukla JP, et al. (2008) Dielectric and optical study of 4-n-decyloxybenzylidene 4.-isopropylaniline exhibiting monotropicsmectic a phase. Macromolecules 4: 73.

10. Lopatina LM, Selinger JV (2009) Theory of ferroelectric nanoparticles in nematic liquid crystals.Phys Rev Lett 102: 197802.

11. Chen HY, Lee W (2005) Electro-optical characteristics of a twisted nematic liquid-crystal cell doped with carbon nanotubes in a DC electric field. Opt Rev 12: 223.

12. ZennyoyiM, Yokoyama J, Takanishi Y, Ishikawa K, Take-zone H, et al. (1998) Dielectric properties in ferroelectric liquid crystal mixtures with ultrashort pitch. J Jap ApplPhys 37: 6071.

13. Naser JA, Himdan TA, Al-Dujaili AH (2014) Synthesis and characterization of Schiff-base liquid crystal containing 1,3,4-oxadizole. International academic research for multidisciplinary 2: 2320.

14. Sileikaite A, Presycevas I, Puiso J, Juraitis A (2006) Analysis of silver nanoparticles produced by chemical reduction of silver salt solution. Mater Sci 12: 287.

15. Lundahl P, Stokes R, Smith E, Martin R, Graham D (2008) Synthesis and characterisation of monodispersed silver nanoparticles with controlled size ranges. Micro & Nano Letters 3: 62.

16. Solomon SD, Bahadory MA, Jeyarajasingam V, Rutkowsky SA, Boritz C, et al. (2007) Synthesis and study of silver nanoparticles. J ChemEdu 84: 322.

17. Majeed Khan MA, Kumar S, Ahamed M, Alrokayan SA, Alsalhi MS (2011) Structural and thermal studies of silver nanoparticles and electrical transport study of their thin films. Nanoscale Res Lett 6: 434.

18. Parmar PR, Mangrola MH, Parmar BH, Josh VG (2012) A Software to Calculate Crystalline Size by Debye-Scherrer Formula Using VB. NET Multi-Disciplinary Edu Global Quest (Quarterly), 1: 1.

19. Houtepen SAA (2010) Dielectric Loss Estimation Using Damped AC Voltages, MSc Thesis, Delft University of Technology, Netherlands.

20. Javed A, Akram M, Shafiq MI (2006) Dielectric properties of cholesterol derivatives. Rom J Phys 51: 819.

21. Manohar R, Srivastava AK, Jyotishman K, Shukla JP, Prajapati AK, et al. (2006) Dielectric, optical and thermodynamical properties of liquid crystal sample exhibiting SmA phase. International Journal of Physical Sciences 3: 147.

22. Ladd MF (1983) Structure and bonding in solid state chemistry, translated by I JSallomi. University of Mosul, Iraq.

23. Tripathi PK, Misra AK, Pandey KK, Manohar R (2013) Study on dielectric and optical properties of ZnO doped nematic liquid crystal in low frequency region. Chemical Rapid Communications 1: 20.

24. Tagir AA (1984) Physical Chemistry of Polymers, translated by A. A. Mohammed. University of Mosul, Iraq.

25. Gornitska OP, Kovalchuk AV, Kovalchuk TN, Kopcansky P, Timko M, et al. (2009) Dielectric properties of nematic liquid crystals with Fe3O4 nanoparticles in direct magnetic field. Semiconductor Physics, Quantum Electronics & Optoelectronics 12: 309.

26. Kumar PP, Yashonath S (2006) Ionic conduction in the solid state. J ChemSci 112: 135.

27. Blinov LM, Chigrinov VG (1994) Electrooptical effect in liqud crystal materials. 1stedn. Springer-Verag, New York, USA.

28. Manohar R, Misra AK, Singh DP, Yadav SP, Tripathi P, et al. (2010) Dielectric, thermal and optical study of an unusually shaped liquid crystal. J PhysChem Solids 71: 1684.

29. Tripathi P, Dixit S, Manohar R (2013) Effect of bridging group on the dielectric properties of liquid crystals. Chemical Rapid Communications 1: 2325.